

# Coherence and correlation of chromatic stellar scintillations in a spaceborne occultation experiment

V. Kan

*A.M. Obukhov Institute of Atmospheric Physics,  
Russian Academy of Sciences, Moscow*

Received June 21, 2004

The model spectra and correlation functions of chromatic stellar scintillations are calculated for synchronous sensing of the Earth's atmosphere at different wavelengths. The model 3D spectrum of air refractivity fluctuations, describing anisotropic and isotropic inhomogeneities, is used. The calculations are performed in the approximations of the equivalent phase screen and weak scintillations. Weak scintillations for low-orbit satellites (Mir station, European ENVISAT/GOMOS satellite) are realized for altitudes of ray perigee above 25–30 km. The scintillation characteristics are shown to depend essentially on the geometry and observation conditions, in the first turn, on the direction of atmospheric sensing. Coherence spectra allow specifying the range of effectively vertical and horizontal sensing angles in atmosphere. The anisotropy coefficient of inhomogeneities can be estimated from autospectra and coherence spectra for effectively horizontal sensing. A set of chromatic scintillation spectra for different atmospheric cross sections allows estimating the main statistical characteristics of atmospheric inhomogeneities in the altitude range 30–70 km. The use of scintillation correlation at different wavelengths allows reducing the errors caused by "scintillation noise" when recovering the concentrations of minor atmospheric constituents in spectrometric star occultation technique. On the basis of analysis of chromatic scintillation spectra and correlation functions, the recommendations for optimum planning of satellite observations are worked out for monitoring of the statistical structure of inhomogeneities and the concentrations of atmospheric constituents.

## Introduction

In recent years, the method based on spaceborne occultation observations of stellar scintillations is actively developed for studying the statistical structure of small-scale density inhomogeneities in the atmosphere.<sup>1–5</sup> Scintillations are understood as relative fluctuations of the received light flux due to light diffraction and refraction at random inhomogeneities.

High sensitivity and spatial resolution of the scintillation method are stipulated by the following circumstances. Since the density quickly decreases with height, scintillations are caused by inhomogeneities located near the ray perigee. The distance between this area and the detector even for low-orbit satellites (Mir station, ENVISAT/GOMOS, UVISI) is several thousands of kilometers. At such a long path, even relatively small density fluctuations lead to significant fluctuations of the received radiation. In this case, the effect of the denser atmospheric layers lying below the ray perigee is excluded.

Spatial resolution of the method is determined by the "thickness" of the sensing beam, whose measure is the radius of the first Fresnel zone. In the optical region, it does not exceed few meters for the spaceborne experiment. In scintillations, the role of smallest-scale inhomogeneities is emphasized; therefore, a fast response of the detector is one of the main requirements in the scintillation method.<sup>4</sup>

Depending on the angular position of a star with respect to the satellite orbit, different trajectories of

its occultation by the atmosphere can be realized: from vertical to tangential. A set of atmospheric cross sections in different directions allows studying the spatial structure of inhomogeneities, their characteristic scales, and anisotropy.

The measurements conducted at Mir station<sup>2–5</sup> have shown that a photometer with the receiving aperture of 20 cm permits reliable measurements of atmospheric scintillations of bright stars at a ray perigee ranging from 70 to 15 km with a spatial resolution up to 1 m. The Tatarskii's theory for weak fluctuations of the radiation transmitted through the randomly inhomogeneous atmosphere provides for rather simple analysis of data in the scintillation method at altitudes above 25–30 km [Refs. 4 and 5]. Below these altitudes, scintillations transit into the mode of strong fluctuations, which complicates their interpretation. In the altitude range and the spatial resolution, the scintillation method surpasses other known contact (balloonborne, airborne, and spaceborne measurement) and remote (radar, lidar) methods.

The advantages achieved in the monitoring of ozone, aerosol, and other atmospheric constituents based on the satellite spectrometric measurements of sun transmittance (a series of SAGE experiments) stimulated the development and carrying out of analogous experiments with the use of stars as radiation sources.<sup>6–8</sup> The use of stars allows the number of observations a day to be increased hundreds times and the information for the whole globe to be obtained. One of the main problems in observing stars is the

problem of scintillations (unlike the sun, for which scintillations are absent).<sup>8,9</sup> Stellar scintillations play the role of some additional multiplicative noise, being one of the main sources of errors in retrieving the content of ozone and other atmospheric constituents.<sup>9,10</sup> For analysis of the structure of scintillations and their correction in spectrometer channels, the GOMOS instrumentation additionally includes two fast photometers.<sup>8</sup>

The first regular observations of stellar scintillations in the Earth's atmosphere were conducted on Salyut-7 and Mir stations.<sup>1-5</sup> In these experiments, two types of stratospheric inhomogeneities were observed: relatively large-scale strongly anisotropic inhomogeneities and isotropic inhomogeneities. Based on the experiments conducted, A.S. Gurvich has developed an empirical model of the 3D spectrum of inhomogeneities of the refractive index, which describes the both types of inhomogeneities.<sup>5,11</sup> The analysis of measurements provided estimates of main parameters of the 3D model spectrum of stratospheric inhomogeneities.<sup>5</sup> The measurements were conducted with a single-frequency photometer. The detailed study of model autospectra of scintillation for different parameters of the 3D model spectrum of inhomogeneities was carried out in Ref. 11.

Synchronous sensing of the atmosphere at different wavelengths opens additional possibilities for studying atmospheric inhomogeneities. The use of the coherence and phase spectra, as well as the correlation functions of chromatic scintillations (fluctuations of light fluxes detected at different wavelengths) allows obtaining additional information about the structure of atmospheric inhomogeneities. In addition, in the spectrometric method of star transmittance,<sup>6-8</sup> the information not only about the amplitude of the scintillation "noise," but also about correlation of scintillations in different spectrometer channels is very important. The use of this information in correction of scintillations<sup>8</sup> and in solution of the inverse problem for retrieving the content of atmospheric constituents<sup>10</sup> considerably reduces the effect of the scintillation noise on the retrieving accuracy.

The objective of this work was the analysis of model coherence spectra and correlation functions of chromatic scintillations in satellite occultation experiment under different observation conditions. A large number of parameters and factors affecting the character of observed scintillations predetermine the variety of possible situations. Therefore, classification and analysis of the most important situations become of primary significance. Our analysis will deal with the retrieval of statistical characteristics of atmospheric inhomogeneities and selection of the optimal observation geometry for obtaining the maximal coherence and the correlation of chromatic scintillations. The calculations are carried out using approximations of weak scintillations and the equivalent phase screen, modeling the atmospheric effect on the propagating radiation. For low-orbit satellites, the approximation of weak scintillations is valid for sensing altitudes of 30 km and higher.

## 1. Atmospheric inhomogeneities and model 3D spectrum

Relative fluctuations of the refractive index  $v = \delta N / \langle N \rangle$  ( $N = n - 1$ ,  $n$  is the refractive index; angular brackets denote statistical averaging) in the optical region are equal to relative fluctuations of air density. Assume that the refractive index for the regular atmosphere ( $N$ ) depends only on the distance from the center of the Earth with the characteristic scale equal to the height of the homogeneous atmosphere  $H_0 = 6-8$  km. The dependence of  $\langle N \rangle$  on the wavelength  $\lambda$  is determined by the dispersion relation, known for air.<sup>12</sup> Horizontal dimensions of the perigee region, significantly affecting the fluctuations of the detected radiation, are several hundreds of kilometers, and the distance from the ray perigee to the low-orbit satellite is several thousands of kilometers. This allows the approximation of the phase screen to be used for the heights of the ray perigee above 25-30 km, assuming only that the phase is modulated at the exit from this region, while intensity fluctuations arise during the ray propagation between the atmosphere and the detector. The characteristics of the statistically inhomogeneous phase screen and conditions of its applicability to the problem under consideration were discussed thoroughly in Refs. 8 and 13.

Observations of stellar scintillations from the Mir station carried out with atmospheric scanning in different directions from the vertical to the horizontal one<sup>1-5</sup> allowed detecting and studying statistical characteristics of two types of inhomogeneities: strongly anisotropic and isotropic. Due to different symmetry, the contribution of anisotropic and isotropic inhomogeneities to resulting scintillations significantly depends on the direction of atmospheric scanning or on the occultation angle  $\alpha$  ( $\alpha$  is the angle between the local vertical and the tangent to the ray trajectory on the phase screen). When the satellite orbiting, the characteristic frequencies of isotropic scintillations are determined by the velocity of ray displacement in the phase screen plane  $v_{\perp}$ , while those of anisotropic scintillations are determined by the vertical component of this velocity  $v_v$ . At  $\alpha = 0^\circ$  the velocities coincide. As  $\alpha$  increases,  $v_v$  decreases and the spectrum of anisotropic scintillations shifts into the low-frequency region. To the contrary,  $v_{\perp}$  increases with the increase of  $\alpha$  and the main part of the amplitude of isotropic scintillations shifts toward the high-frequency region. This frequency selection of anisotropic and isotropic scintillations for  $\alpha \neq 0^\circ$  allows the contributions to the resulting scintillations to be separated. A high speed of the photometer used in Refs. 2-5 with the signal sampling frequency up to 16 kHz permitted the characteristics of not only anisotropic, but also isotropic scintillations to be studied.

The statistical properties of a random medium for the problems of light propagation are described by the 3D spatial spectrum  $\Phi_v$  of relative fluctuations

of the refractive index.<sup>14</sup> Based on the observations of stellar scintillations, Gurvich has developed the model of  $\Phi_v$  and retrieved the statistical characteristics of anisotropic and isotropic inhomogeneities in the altitude range 25–70 km [Refs. 3, 5, and 11]. This model is based on the assumption of statistical independence of the isotropic and anisotropic components of atmospheric inhomogeneities:

$$\Phi_v = \Phi_W + \Phi_K, \quad (1)$$

where  $\Phi_W$  is the spectral component describing anisotropic inhomogeneities, while  $\Phi_K$  describes isotropic ones. Assuming that the isotropic inhomogeneities are caused by the Kolmogorov turbulence,  $\Phi_K$  can be written in the form<sup>14</sup>:

$$\Phi_K(\kappa) = 0.033C_K\kappa^{-11/3}\phi_K(\kappa/\kappa_m), \quad (2)$$

where  $C_K$  is the structure characteristic;  $\kappa = \sqrt{\kappa_x^2 + \kappa_y^2 + \kappa_z^2}$ ,  $\kappa_z$  is the vertical wave number,  $\kappa_x$  and  $\kappa_y$  are the horizontal wave numbers ( $\kappa_x$  is directed along the ray direction;  $\kappa_y$  is directed along the tangent to the Earth's limb);  $\kappa_m = 5.92/l_K$ ,  $l_K$  is the inner scale of turbulence. The function  $\phi_K(\kappa/\kappa_m)$  describes the decay in the region of molecular viscosity, and we define it in the form of the Gaussian function.<sup>14</sup>

The observations of stellar scintillations<sup>1–5</sup> show that the anisotropic component can be described within the framework of the model of saturated inner waves, for which the 3D spectrum can be written in the form<sup>5,11</sup>:

$$\Phi_W = C_W\eta^2(\kappa^2 + \kappa_0^2)^{-5/2}\phi_W(\kappa/\kappa_W); \quad \kappa = \sqrt{\eta^2\kappa_\perp^2 + \kappa_z^2}, \quad (3)$$

where  $C_W$  is the analog of the structure characteristic;  $\eta$  is the anisotropy coefficient;  $\kappa_\perp = \sqrt{\kappa_x^2 + \kappa_y^2}$ ,  $\kappa_0 = 2\pi/L_0$ , and  $L_0$  is the vertical outer scale of inhomogeneities,  $\kappa_W = 2\pi/l_W$  and  $l_W$  is the scale of "turbulent viscosity" (inner scale) of anisotropic inhomogeneities. For simplification of the calculations, we will use the Gaussian function for a function  $\phi_W$ , describing the decay of the spectrum in the small-scale range, in the horizontal wave numbers and the power function of the form  $(1 + \kappa_z^2/\kappa_W^2)^{-1}$ , which is in a better agreement with the measurements,<sup>3,5</sup> in the vertical wave numbers.

The model 3D spectrum (1)–(3) is determined by the following basic parameters: the structure characteristics  $C_W$  and  $C_K$ , the characteristic inner scales of inhomogeneities  $l_W$  and  $l_K$ , the outer scale  $L_0$ , and the anisotropy coefficient  $\eta$  for the anisotropic component of the spectrum. The scintillations for the Kolmogorov component of the spectrum are insensitive to the outer scale of inhomogeneities.<sup>14</sup> In analysis, we should also take into account the parameters, determining the conditions of measurements and the receiving aperture. The most important among them, as was shown in Refs. 4, 5, 8, and 11, are: the occultation angle  $\alpha$ , the wavelengths  $\lambda_1$  and  $\lambda_2$ , the

effective wavelength bands of the received radiation  $\Delta\lambda_1$  and  $\Delta\lambda_2$ , the sampling frequency, and the time of signal accumulation in a sample  $\tau$ , as well as characteristics of measurement noise. In the analysis, we will use the characteristics of GOMOS fast photometers as basic instrument parameters. Remind that for them  $\lambda_1 = 495$  nm and  $\lambda_2 = 675$  nm, the passbands of the optical filters  $\Delta\lambda_1 = \Delta\lambda_2 = 50$  nm,  $\tau = 1$  ms (the sampling frequency of 1000 Hz). The occultation angle  $\alpha$  can vary from 0 to 90°.

The chromatic effects in scintillations upon transmission are caused by the following circumstances. Because of the dispersion of the regular atmospheric refraction, the rays  $\lambda_1$  and  $\lambda_2$ , separated vertically in the atmosphere,<sup>8</sup> arrive at the detection point at the same time. The chromatic shift of the rays  $\Delta\lambda$  is determined by the wavelengths and the height of the ray perigee. If radiation is detected in some effective filter bands  $\Delta\lambda_1$  and  $\Delta\lambda_2$ , then it is additionally smoothed in the corresponding vertical scales of the filters  $\Delta p_1$  and  $\Delta p_2$  [Refs. 8 and 11]. For the vertical and close-to-vertical atmospheric cross sections, the filters smooth high-frequency scintillations. For the close-to-horizontal cross sections, the filters reduce the scintillation amplitude, but the high-frequency structure of scintillations keeps unchanged. In addition, the wavelength difference leads to the different diffraction effects during the propagation, in particular, to the diffraction decorrelation of scintillations. The chromatic shift and the effect of filters were considered in detail in Refs. 4, 8, and 11.

The analysis of the problem under consideration becomes considerably more simple, when restricted to the condition of weak scintillations. This condition takes place when relative variances of isotropic and anisotropic scintillations are small as compared to unity.<sup>14</sup> In this case, the correlation functions and the scintillation spectra for the model (1) can also be represented as sums of isotropic and anisotropic scintillation components.<sup>5</sup> The experimental data can be used directly to estimate the 1D spectra and the correlation functions of chromatic scintillations along some part of the trajectory of observations. All the equations needed in calculating the 1D mutual spectra and mutual correlation functions of chromatic scintillations by the given model 3D spectrum of atmospheric inhomogeneities, taking into account the filters and the time of signal accumulation, are presented in Refs. 5, 8, and 11. These equations are quite cumbersome and therefore omitted here. Note only that the transition from the measured temporal (frequency) dependences to the spatial wave numbers is performed based on the hypothesis of frozen turbulence.<sup>14</sup> First, we will consider the properties of anisotropic and isotropic scintillations separately and then the properties of the resulting scintillations.

## 2. Anisotropic scintillations

The vertical inner scale  $l_W$  in the altitude range 30–70 km somewhat increases with height and ranges

mostly from ten to hundred meters.<sup>5</sup> The values of  $l_W$  significantly exceed the vertical dimension of the first Fresnel zone

$$\rho_F = \sqrt{2\pi q \lambda L} \approx 3 \text{ m}$$

( $q$  is the coefficient of regular refraction extinction and  $q = 0.7-1.0$  in the altitude range of interest;  $L \approx 2000-3500$  km is the distance from the phase screen plane to an observer). Therefore, the diffraction effects are insignificant for anisotropic scintillations. In addition, if filter passbands are rather narrow,  $l_W$  is also greater than the vertical averaging scales of the filters  $\Delta p_1$  and  $\Delta p_2$  [Ref. 8] (for fast GOMOS photometers,  $\Delta p_1$  and  $\Delta p_2$  do not exceed 5 m for the altitudes above 30 km), and therefore,  $l_W$  is the main scale for anisotropic scintillations.<sup>8</sup> The outer scale  $L_0$  determines the saturation of the spectrum of inhomogeneities  $\Phi_W$  in the region of low frequencies. Following Ref. 15, we assume that it is connected with  $l_W$  through some coefficient. The anisotropy coefficient is one of the most important and, at the same time, one of the most poorly studied parameters. The observations of stellar scintillations at skew occultations<sup>1</sup> yielded the following estimate:  $\eta > 25$ . The information about the anisotropy coefficient is contained explicitly in the observations of tangential occultations. In the case of tangential occultation, the star descends to the height  $h_{\min}$  and then, not disappearing behind the horizon, rises again. In some area near  $h_{\min}$ , the star moves practically parallel to the Earth's limb, thus scanning horizontally atmospheric inhomogeneities. For two tangential observations,<sup>16,17</sup> the estimate  $\eta \approx 100$  was obtained from the autospectra of scintillations at some simplifying assumptions. As will be shown below, using the coherence spectra of scintillations, it is possible to obtain more correct estimates of the anisotropy coefficient.

An important integral parameter of the problem is the dispersion shift between rays  $\Delta_A$  in the phase screen plane. The altitude dependence of  $\Delta_A$  for the fast GOMOS photometers is presented in Ref. 8. Its values, depending on the wavelengths and proportional to their difference, increase almost exponentially with the decrease of altitude for the perigee heights above 30 km. Below 30 km,  $\Delta_A$  for the fast GOMOS photometers saturates slowly roughly to 100 m. Note that, according to the model of the standard atmosphere,  $\Delta_A = 9.9$  m for the perigee height of 30 km and  $\Delta_A = 2.3$  m for the height of 40 km. Since the diffraction effects are insignificant for anisotropic scintillations,  $\Delta_A$  plays the role of the main factor, causing decorrelation of scintillations at different wavelengths.

Depending on  $\alpha$ , occultations can be conditionally divided into two categories: effectively vertical and horizontal. The condition for the effectively vertical occultations for anisotropic inhomogeneities, obtained from simple qualitative reasoning, can be written in the form<sup>8</sup>:

$$\tan \alpha < G_W \equiv \eta \frac{l_a^*}{2\pi \Delta_A + l_a^*}, \quad (4)$$

where  $l_a^*$  is the characteristic vertical scale of inhomogeneities, being the main contributors to the amplitude of scintillations. If the condition (4) is fulfilled, we can believe that, at the perigee height above 30 km, the both rays mostly intersect the same inhomogeneities in the atmosphere (with a height or time shift) and the scintillations are fully determined by the vertical structure of inhomogeneities only. In this case, the coherence and the correlation of scintillations at different wavelengths are close to maximum. As  $\alpha$  increases, the condition (4) is violated, starting from small-scale inhomogeneities. Correspondingly, the coherence of scintillations at different wavelengths breaks down, in the first turn, in the high-frequency region. For the fast GOMOS photometers, the role of  $l_a^*$  is played by the inner scale  $l_W$ . In this case, the characteristic frequency of scintillations in the high-frequency region is determined by  $l_W$ . If signals are averaged over rather large intervals  $\Delta t_{av}$  (as, e.g., in UVISI<sup>6</sup> and ENVISAT/GOMOS<sup>7,8</sup> spectrometric channels with  $\Delta t_{av} = 0.25-0.5$  s), then in this case the role of the "correlating" scale  $l_a^*$  for anisotropic scintillations is played by the vertical averaging scale  $v_v \Delta t_{av}$  [Ref. 8]. Since this averaging scale is usually much greater than  $l_W$ , the range of effectively vertical angles with high values of coherence and correlation extends additionally in accordance with Eq. (4). For vertical occultations, the scintillations do not explicitly contain the information about  $\eta$ .

If the inequality opposing to the inequality (4) is true, occultations can be considered as effectively horizontal. In this case, the coherence and the correlation of scintillations at different wavelengths for the fast photometers significantly depend on the relation between the scales  $l_W$  and  $\Delta_A$ . If the vertical separation between the rays  $\Delta_A$  exceeds the "correlating" scale  $l_W$ , then the coherence and correlation for the horizontal scanning are much smaller than those for the vertical scanning.

Figure 1 shows the 1D model autospectra, coherence spectra, and normalized mutual correlation functions of chromatic scintillations. For the spectra the abscissa is the normalized vertical wave number  $\kappa_{zn} = \kappa_z / \kappa_W$ , and for the correlation function it is the vertical shift  $\Delta h$  between the signals  $\lambda_1$  and  $\lambda_2$ , inputted into the photometer channel  $\lambda_1$ . The autospectra (they are shown only for  $\lambda_1$ ) are presented as a dimensionless product of the wave number by the spectral density of scintillations  $\kappa_{zn} \cdot V_J(\kappa_{zn}, \lambda_1)$ . The coherence spectra are given in the form

$$\text{coh}(\kappa_{zn}, \lambda_1, \lambda_2) = |V_J(\kappa_{zn}, \lambda_1, \lambda_2)|^2 / V_J(\kappa_{zn}, \lambda_1) V_J(\kappa_{zn}, \lambda_2),$$

where  $V_J(\kappa_{zn}, \lambda_1)$  and  $V_J(\kappa_{zn}, \lambda_2)$  are autospectral, and  $V_J(\kappa_{zn}, \lambda_1, \lambda_2)$  is the mutual spectral density of scintillations at different wavelengths.

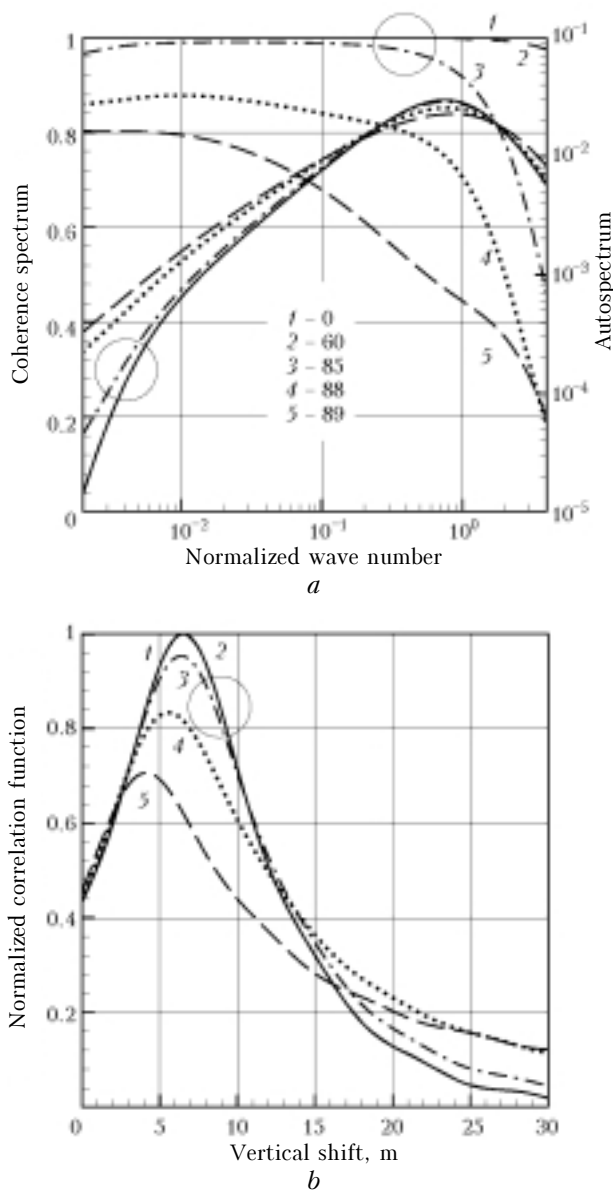


**Fig. 1.** Coherence spectra (curves 1–5), autospectra (a) and normalized correlation functions (b) of anisotropic chromatic scintillations for effectively vertical occultations, as well as the occultation angles (deg.) for the spectra and correlation functions.

The normalized mutual correlation function is presented in the form

$$R(\Delta h, \lambda_1, \lambda_2) = \langle \delta J(h, \lambda_1) \delta J(h + \Delta h, \lambda_2) \rangle / \sqrt{\langle \delta J^2(h, \lambda_1) \rangle \langle \delta J^2(h, \lambda_2) \rangle},$$

where  $\delta J$  are relative fluctuations of the detected light flux at a corresponding wavelength. The mutual correlation function

$$B(\Delta h, \lambda_1, \lambda_2) = \langle \delta J(h, \lambda_1) \delta J(h + \Delta h, \lambda_2) \rangle$$

is related to the mutual spectrum  $V_f(\kappa_{zn}, \lambda_1, \lambda_2)$  through Fourier transforms.<sup>18</sup> The calculations are

performed for the following conditions: the radiation is monochromatic ( $\Delta\lambda_1 = \Delta\lambda_2 = 0$ ) at  $\lambda_1 = 495$  nm and  $\lambda_2 = 675$  nm, the ray perigee height  $h = 33$  km (for this height  $\Delta_A = 6.5$  m),  $\eta = 30$ ,  $l_W = 30$  m,  $L_0/l_W = 300$ .

It is seen from Fig. 1 that if the inequality (4) is true, occultations can be interpreted as effectively vertical (for the chosen conditions, these occultations are with  $\alpha \leq 85^\circ$ ; the corresponding curves are enclosed by circles). The autospectra are close to each other, and the coherence and the maxima of the correlation functions  $R_{\max}$  are close to unity. The high-frequency decay boundary of autospectra is determined by  $l_W$ . This scale also determines the correlation length of chromatic scintillations. The maximum of  $R_{\max}$  is observed at full compensation for the chromatic shift between  $\lambda_1$  and  $\lambda_2$ :  $\Delta h_{\max} = \Delta_A$ . The decay of autospectra in the low-frequency (large-scale) region is caused by  $L_0$  [Ref. 15]. The character of this decay and the value of the boundary frequency depend on the method of introduction of the outer scale into the model 3D spectrum  $\Phi_W$ .

The structure characteristic  $C_W$  is included in the form of the coefficient of proportionality for the autospectrum amplitude.<sup>8,11</sup> The dependence on  $\eta$  manifests itself in the nonlinear dependence of the amplitudes of autospectra on  $\eta$ . They increase roughly proportionally to  $\eta$  for  $\eta < 30$  and saturate quickly for  $\eta > 30$  (transition to spherically stratified inhomogeneities).<sup>11</sup>

As the occultation angle increases ( $\alpha > 85^\circ$ ), the behavior of the curves changes. The information about the outer scale disappears from the autospectra. The coherence and the maxima of the correlation function decrease fast, and the position of  $R_{\max}$  displaces.

Thus, the high level of coherence and  $R_{\max}$  of scintillations at different wavelengths can serve a criterion of the condition (4) of the effectively vertical occultation. In this case, for anisotropic inhomogeneities it is possible to estimate the following parameters of  $\Phi_W$ : the inner  $l_W$  and outer  $L_0$  scales of inhomogeneities from the characteristic decay frequencies of the autospectra; the structure characteristic  $C_W$  (if the estimate of  $\eta$  is known). In addition, it is possible to determine  $\Delta_A$ , which can be used, in particular, to retrieve the regular vertical profile of the refractive index on the assumption of the local spherical symmetry of its distribution, using the Abel inversion.<sup>8</sup>

Note that the dispersion shift can also be determined from the phase spectrum of chromatic scintillations.<sup>8</sup> Here we consider the correlation of scintillations because of its importance for problems of retrieving the content of ozone and other atmospheric constituents in spectrometric observations.<sup>8–10</sup> Without additional *a priori* information, it is impossible to determine the anisotropy coefficient only from the vertical occultations.

Consider the possibility of estimating  $\eta$  from the data of tangential occultations. In this case, at the effectively horizontal part of the realization, the characteristic frequencies of the scintillation autospectra are determined by the "horizontal" inner

scale of inhomogeneities  $\eta l_W$ . As was already mentioned above, the coherence of scintillations at different wavelengths in the case of horizontal scanning significantly depends on the relation between the scales  $l_W$  and  $\Delta_\lambda$ . Thus, it becomes possible to estimate independently  $l_W$  from the coherence spectrum. Given the estimate of  $l_W$ , we can determine  $\eta$  by separating the characteristic scale  $\eta l_W$ .

For the altitude of 33 km, Fig. 2 shows the coherence spectra versus the normalized horizontal wave numbers  $\kappa_y \eta l_W / 2\pi$ . It is seen from Fig. 2a that, in some range of the occultation angles ( $\tan \alpha \geq 10C_W$ , curves are enclosed by a circle), the coherence spectra keeps their shape and almost coincide for  $\eta = 10$  and 100. The parts of the trajectories, falling within this range of the angles, can be considered as effectively horizontal, and the spectral amplitudes of coherence are minimal in this case. For the considered conditions, they correspond to  $\alpha = 90-88.3^\circ$  for  $\eta = 10$  and  $\alpha = 90-89.8^\circ$  for  $\eta = 100$ . Note that for the tangential GOMOS occultations, these angles correspond to the trajectory parts about 1000 and 150 km long, respectively, on the both side from the point of minimum  $h_{\min}$ . As the trajectory deviates from effectively horizontal ( $\alpha$  decreases), the coherence spectra change quickly.

In Fig. 2b, it is shown that the "horizontal" coherence spectra depend strongly on  $l_W$  (rather, on the ratio between  $\Delta_\lambda$  and  $l_W$ ). The coherence spectra change most significantly, when the values of the "correlating"  $l_W$  and the "decorrelating" scale  $2\pi\Delta_\lambda$  are comparable ( $l_W = 10-50$  m in Fig. 2). For fast GOMOS photometers, the altitude range 30-40 km meets this condition.<sup>5,8</sup>

The circumstance that the coherence spectra for the effectively horizontal scanning depend strongly on  $l_W$  and, at the same time, have low sensitivity to  $\eta$  allows estimating  $l_W$  from them. For this purpose, the values of  $\Delta_\lambda$  from the model of the standard atmosphere can be used, because the variations of the regular profile of the refractive index (and, consequently,  $\Delta_\lambda$ ) can be neglected when estimating  $\eta$ . Then, using the estimate of the characteristic horizontal scale  $\eta l_W$  obtained from the autospectra, it is possible to find  $\eta$ . At the same time, the outer scale cannot be estimated from horizontal observations.

The effectively horizontal scanning is realized near  $h_{\min}$ , and all the retrieved parameters of  $\Phi_W$  correspond to this height. Therefore, it seems interesting to conduct a cycle of tangential observations of the same star at the satellite sequential orbit passes. Due to the orbit precession,  $h_{\min}$  will increase (or decrease) at every following pass, thus providing the vertical set of horizontal cross sections of the atmosphere. The set of effectively vertical and tangential occultations allows all the parameters of  $\Phi_W$  to be determined.

The effect of filters becomes significant in the case, when the vertical averaging scales of the filters  $\Delta p_1$  and  $\Delta p_2$  are comparable with or exceeding  $l_W$  (low altitudes and/or wide filter passbands).<sup>8,11</sup> In

the case of fast GOMOS photometers, the effect of the filters becomes considerable for the sensing altitudes below 30-35 km.

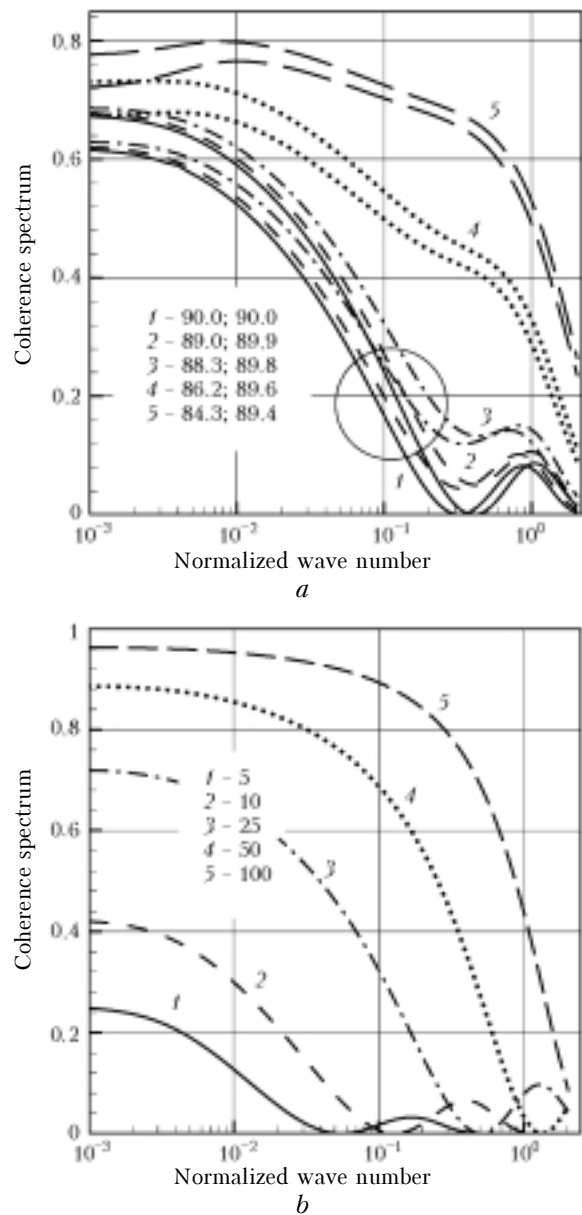


**Fig. 2.** Coherence spectra of anisotropic chromatic scintillations for tangential occultations: (a) calculation for the anisotropy coefficient  $\eta = 10$  (occultation angles (deg.) shown in the first column in the inset) and  $\eta = 100$  (occultation angles in the second column);  $l_W = 20$  m; curves for  $\eta = 100$  lie above the similar curves for  $\eta = 10$ ; (b) calculation at  $\alpha = 90^\circ$  for different inner scales  $l_W$  (values of  $l_W$ , in m, are given in the inset).

Here we do not discuss the problem of correction of the measurement noise in detail. Note only that, using the calibration records of star radiation outside the atmosphere (at the altitudes of about 100 km and higher), for the photodetector shot noise, described by the Poisson law, it is possible to estimate all the needed statistical moments of noise for atmospheric

measurements. The practical application of this procedure and the characteristic parameters of noise at observations of scintillations are given in Refs. 1–5. The statistical error of noise correction in autospectra is determined by the lengths of realizations used to estimate the noise and autospectra. The mutual spectrum  $V_j(\kappa, \lambda_1, \lambda_2)$  and the mutual correlation function  $B(\Delta h, \lambda_1, \lambda_2)$  of chromatic scintillations are independent of the quantum noise. Autospectra and variances of scintillations, which are used for normalization, introduce the residual error of noise correction to the coherence spectrum  $\text{coh}$  and the normalized correlation function  $R$ . The noise level is determined by the brightness of the observed star, and the scintillation/noise ratio depends on the sensing height. The effect of noise is more significant for high perigee heights (45–50 km and higher), where its level is comparable with scintillations. With the decrease of height, the relative amplitude of scintillations increases roughly exponentially, while that of noise increases in the inverse proportion to the mean signal intensity, and therefore the effect of noise decreases. At low heights (below 20–25 km), the role of noise increases again due to considerable attenuation of radiation in the atmosphere and saturation of scintillations in the mode of strong fluctuations.

### 3. Isotropic scintillations

The outer scale of the Kolmogorov turbulence does not manifest itself in the scintillation spectra.<sup>14,19</sup> For the chosen model spectrum  $\Phi_K$ , the parameters, which can be retrieved from observations of scintillations, are the structure characteristic  $C_K$  and the inner scale  $l_K$  [Refs. 5 and 11]. The characteristic values of the inner scale in the stratosphere range from several decimeters to several meters, increasing with height.<sup>5</sup> These values are comparable with or even smaller than the radius of the Fresnel zone  $\rho_F$ . Therefore, diffraction effects are significant for isotropic scintillations. The role of the "correlating" scale  $l_i^*$  for chromatic scintillations is played by  $\rho_F$  (or  $l_K$ , if  $l_K > \rho_F$ , or their combination), because inhomogeneities at the scales  $\rho_F$  and/or  $l_K$  are the main contributors to the amplitude of isotropic scintillations.<sup>8,14</sup> The "decorrelating" scale is still the chromatic shift  $\Delta_\lambda$ . If the scintillations at any wavelength (1D spatial autospectra) are independent of the direction of atmospheric scanning due to the isotropy of inhomogeneities, then the correlation and coherence of scintillations at different wavelengths depend significantly on the occultation angle. This is connected with the fact that the chromatic shift occurs along the separated direction, namely, the local vertical. For isotropic inhomogeneities, the maximum of correlation is observed, when  $\lambda_1$  and  $\lambda_2$  correspond to the minimal separation between the rays  $l_{\min} = \Delta_\lambda \sin \alpha$ . The coherence and correlation of chromatic scintillations are high, if the occultations are close to vertical  $\alpha \approx 0^\circ$  and the both rays sequentially intersect

the same inhomogeneities. By analogy with the previous case, these occultations will be referred to as effectively vertical. In this case, the decorrelation is determined by the diffraction effects or by the different scales of the filters  $\Delta p_1$  and  $\Delta p_2$ . For skew occultations, if the "correlating" scale  $l_i^*$  is smaller than  $l_{\min}$ , the rays intersect different inhomogeneities and the coherence decreases fast as  $\alpha$  increases.

The condition of "verticality" for the occultation angles and isotropic inhomogeneities can be obtained from the condition that  $l_{\min} < l_i^*$  and written in the form similar to Eq. (4):

$$\sin \alpha < G_K \equiv l_i^* / (2\pi \Delta_\lambda). \quad (5)$$

The condition (5) imposes much more rigorous restrictions on the range of angles, for which the coherence and the correlation are quite significant. This is connected with the fact that not only  $\eta = 1$ , but also  $\rho_F$  and  $l_K$  are much smaller than  $l_W$ . The condition (5) [as well as Eq. (4)] should take into account the effects connected with the displacement of inhomogeneities normally to the ray because of the rotation of the atmosphere together with the Earth. These effects depend on the orientation of the satellite orbit and the observed star and achieve the maximum when the phase screen plane coincides with the plane of celestial equator. In this case, the corrections to the occultation angle can be as large as  $9^\circ$ . To be noted is also the following principal difference of the conditions (4) and (5). For isotropic inhomogeneities, the role of the "correlating" scale is always played by  $\rho_F$  (or  $l_K$ ), because scintillations in the entire spectrum of scales are determined by the smallest-scale inhomogeneities.<sup>8,14</sup> Therefore, for the Kolmogorov turbulence, in contrast to anisotropic inhomogeneities, the time averaging of signals in spectrometric (low-frequency) channels of the UVISI and ENVISAT/GOMOS spectrometers does not lead to the extended range of the occultation angles with the high values of coherence and correlation.<sup>8</sup>

Figure 3a shows the coherence spectra of the monochromatic radiation at  $\lambda_1 = 495$  nm and  $\lambda_2 = 675$  nm for two heights. The occultation angles  $\alpha$  for 30 km are re-calculated from the data for 40 km in accordance with Eq. (5), and the corresponding coherence spectra almost coincide. For comparison, the curves for 40 km with  $l_K = 5$  m are shown as well. Figure 3b depicts the normalized mutual correlation functions  $R$  for 40 km as calculated for the fast GOMOS photometers and for the monochromatic radiation at  $\lambda_1$  and  $\lambda_2$ . It can be seen from Fig. 3 that the coherence and the correlation decrease quickly as the occultation deviates from the vertical by only a few degrees, whereas for anisotropic inhomogeneities the range of effectively vertical angles extends to  $85^\circ$  (see Fig. 1). The introduction of the inner scale  $l_K = 5$  m (in Fig. 3a) leads to a marked increase of the coherence: at  $\alpha = 0^\circ$   $\text{coh} \approx 1$ , which corresponds to transition to the geometric-optics approximation  $l_K \gg \rho_F$ .

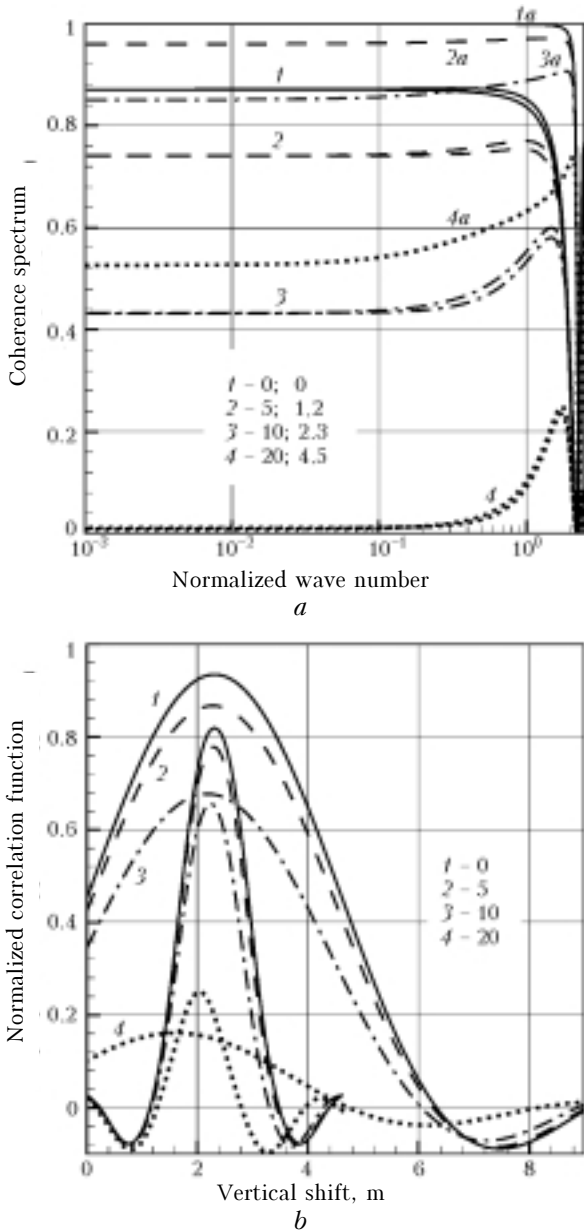


**Fig. 3.** Coherence spectra and correlation functions of isotropic chromatic scintillations: (a) curves 1–4 are the coherence spectra for two monochromatic radiations with the inner scale  $l_K = 0$  m for the height of 30 km (occultation angles (deg.) in the first column in the inset) and 40 km (occultation angles in the second column); curves 1a–4a correspond to the calculations for 40 km with  $l_K = 5$  m; (b) curves 1–4 are the calculations at  $h = 40$  km for the conditions of the fast GOMOS photometers (occultation angles (deg.) in the inset); unlabelled curves are the calculations for two monochromatic radiations.

The form of the correlation functions  $R$  for the monochromatic radiations  $\lambda_1$  and  $\lambda_2$  at  $l_K = 0$  m (Fig. 3b, unlabelled curves) is fully determined by the diffraction effects. Correspondingly, the correlation length in this approximation is determined by  $\rho_F$  and almost independent of height. The difference of  $R_{max}$  from unity is caused by the diffraction decorrelation.  $R_{max}$  is observed at the vertical shift

$\Delta h_{max} = \Delta_A \cos^2 \alpha$ , which corresponds to the minimal separation between the ray trajectories  $l_{min} = \Delta_A \sin \alpha$ . This shift with the factor  $\cos^2 \alpha$  (as compared to anisotropic scintillations) is seen in the figure for  $\alpha = 20^\circ$ . The time shift is, correspondingly, equal to  $\Delta t_{max} = (\Delta_A/v_v) \cos^2 \alpha$ . As was mentioned above, the filters and the time of signal accumulation  $\tau$  in a sample can play a significant role for isotropic scintillations. The effects of the filters and the accumulation time manifest themselves in different ways, because the filters provide averaging along the vertical, while the time accumulation performs averaging along the ray trajectory. Both these effects lead to the broadening of the correlation functions  $R$ , and the filters additionally shift  $R_{max}$  for occultations deviating from vertical ones. The effect of the filters increases sharply with the decreasing height (the scales of  $\Delta p_1$  and  $\Delta p_2$  increase roughly exponentially with the decreasing height), while the vertical averaging scale is almost independent of height. The labeled curves in Fig. 3b show  $R$  calculated for the conditions of the fast GOMOS photometers at an altitude of 40 km. At this altitude, the main effects (broadening of  $R$ , increase of  $R_{max}$  for small  $\alpha$ ) are caused by averaging of signals at  $\tau = 1$  ms. For altitudes of 35 km and lower, the filters exert the principal effect on the signals of the GOMOS photometers.

#### 4. Scintillations for a two-component model

Using the autospectra  $fV_j(f, \lambda_1)$  as an example, consider first the above effects of the frequency selection and the filters in the resulting scintillations.<sup>11</sup> Figure 4a demonstrates these effects for the height of 33 km. The calculation was performed for the following parameters of the model 3D spectrum:  $l_W = 30$  m,  $\eta = 30$ ,  $l_K = 0$ ; the structure characteristics  $C_W$  and  $C_K$  were taken equal to their average values at this height as obtained from the experiment.<sup>5</sup> The unlabelled curves show the effect of frequency separation of the anisotropic (low-frequency) and isotropic (high-frequency) monochromatic scintillations at the occultation angle increase. The detection of radiation in the finite filter passband (labeled curves) for close-to-vertical occultations mostly smoothes the high-frequency components of the scintillations. The scale and the characteristic frequency of smoothing are determined by the scales of  $\Delta p_1$  and  $\Delta p_2$ . For skew occultations with  $\alpha \geq 60^\circ$ , the filters lead to a significant decrease of spectral amplitudes of isotropic scintillations. It should be also taken into account that the finite time  $\tau$  of signal accumulation during sampling ( $\tau = 1$  ms and the Nyquist frequency is 500 Hz for the fast GOMOS photometers) leads to smoothing of high-frequency scintillations. For skew occultations, this additionally decreases the weight (variance) of isotropic (uncorrelated) scintillations, increasing  $R_{max}$ .

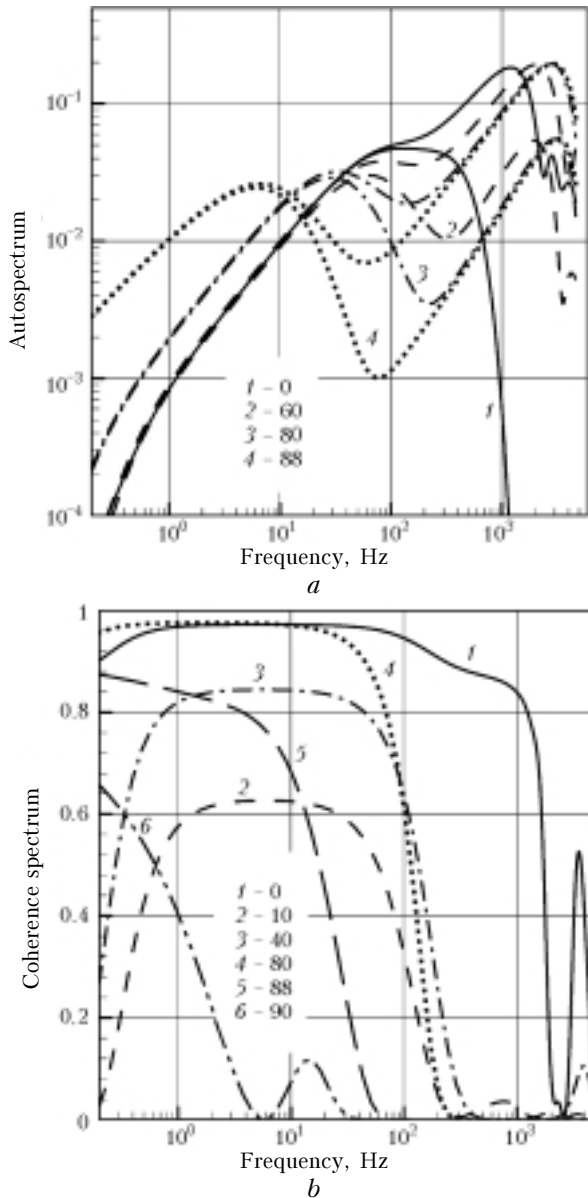


**Fig. 4.** Autospectra and coherence spectra of chromatic scintillations for a two-component model of the 3D spectrum of inhomogeneities: (a) autospectra for two monochromatic radiations and in the filter passbands (the latter are marked by digits 1–4); (b) coherence spectra in the filter passband; the corresponding occultation angles (deg.) are given in the inset.

Using the occultation with  $\alpha = 80^\circ$  (labeled curve 3 in Fig. 4a) as an example, consider the behavior of the spectrum of resulting scintillations in more detail. The low-frequency component of the autospectrum is mostly represented by anisotropic scintillations. The frequency of its maximum is determined by the inner scale of anisotropic inhomogeneities  $l_w$ :  $f_a^* \propto v_v / l_w$ . The frequency, at which the autospectrum deviates from the linear dependence in the low-frequency region, is determined by the outer scale  $L_0$ . The spectral amplitudes are determined by the structure characteristic  $C_w$ , and, in addition, they depend on the anisotropy coefficient  $\eta$  [Ref. 11]. The isotropic scintillations

determine the high-frequency component of the autospectrum. The frequency of its maximum is determined by the radius of the Fresnel zone  $\rho_F$ :  $f_i^* \propto v_L / \rho_F$  (or the inner scale of the Kolmogorov turbulence  $l_K$ , if  $l_K \geq \rho_F$ ). The spectral amplitudes are determined by the structure characteristic  $C_K$ , as well as by the inner scale  $l_K$ , if  $l_K \geq \rho_F$  [Refs. 11 and 14].

Figure 4b shows the calculated coherence spectra for  $\lambda_1 = 495$ ,  $\lambda_2 = 675$  nm, and the passbands  $\Delta\lambda_1 = \Delta\lambda_2 = 50$  nm for a height of 33 km. The coherence is maximal for the purely vertical occultation  $\alpha = 0^\circ$  (curve 1), at which both components of scintillations: anisotropic and isotropic, are characterized by the highest coherence. The difference of  $\text{coh}(f)$  from unity is connected both with the different scales of  $\Delta p_1$  and  $\Delta p_2$  and with the diffraction effects for the isotropic component of scintillations. However, already at  $\alpha = 10^\circ$  (curve 2) the resultant coherence decreases drastically because the isotropic scintillations become incoherent and contribute to the resultant scintillations as an uncorrelated noise. As the occultation angle increases (curves 3 and 4), the coherence increases again, because the anisotropic scintillations still have high coherence and the weight of the isotropic (incoherent) scintillations decreases progressively due to the frequency selection and suppression by the filters. It can be noted that at  $\alpha = 80^\circ$  the effect of the isotropic component on the resultant coherence is rather low and the coherence is close to that given by the purely anisotropic scintillations. The frequency range, in which the coherence is significant, corresponds to the frequency range of anisotropic scintillations. At further increase of the angle  $\alpha = 88^\circ$ , the coherence decreases, because these angles are already beyond the range of effectively vertical angles for anisotropic inhomogeneities, as is seen from Fig. 1 (when comparing, it should be kept in mind that in Fig. 1 the spatial frequency is plotted as an abscissa). At  $\alpha = 90^\circ$ , the coherence is minimal and its spectrum has the form characteristic of horizontal cross sections (see Fig. 2).

The calculations of the correlation functions show that the highest values of  $R_{\max}$  are achieved at the close-to-vertical occultations at  $\alpha \approx 0^\circ$ , for which the both components of the scintillations are maximally correlated. The correlation length in this case is minimal, because a significant contribution is due to the isotropic component, whose correlation length is much smaller than that of the anisotropic component. As the occultation angle deviates by a few degrees from the vertical, the correlation of the resultant scintillations is mostly determined by the anisotropic component alone. In this case, the correlation length increases and is determined by  $l_w$ .

The dependence of  $R_{\max}$  on the occultation angle for the fast GOMOS photometers is shown in Fig. 5. For comparison, the analogous dependence with the increased weight of the isotropic component is shown as well. Let us analyze this dependence from the viewpoint of achieving maximal correlation of scintillations at different wavelengths.

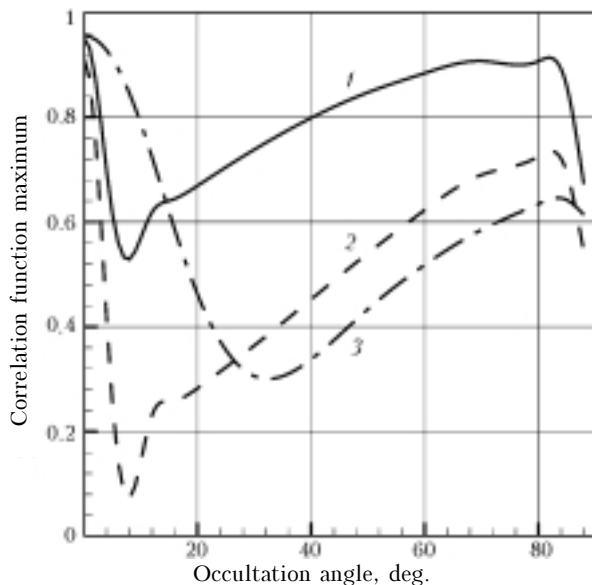


**Fig. 5.** Maxima of the mutual correlation functions of chromatic scintillations for the conditions of measurement with the fast GOMOS photometers: (1) the ray perigee height of 30 km at the average weight ratio of the anisotropic and isotropic scintillations; (2) height of 30 km at the fivefold increased weight of the isotropic component; (3) height of 40 km at the average weight ratio.

For occultations very close to vertical ( $\alpha < 5\text{--}10^\circ$  for 40 km and  $\alpha < 1\text{--}2^\circ$  for 30 km), both the anisotropic and isotropic components of scintillations are well correlated. In addition, in this range of angles, the correlation length is minimal, which increases the accuracy of determination of the  $R_{\max}$  position. The values of  $R_{\max}$  are the largest, and this range is the best for the problem at hand. However, this range is very narrow and the number of rather bright stars, falling within this range, is knowingly insufficient for the purposes of monitoring. When planning experiments and analyzing the data in this range of the occultation angles, one should take into account the shift of atmospheric inhomogeneities in the direction perpendicular to the ray due to the Earth's rotation. In the intermediate range  $5\text{--}10 \leq \alpha < 30\text{--}45^\circ$ , anisotropic scintillations are still highly correlated, but the isotropic ones are already uncorrelated. In this range of angles, the isotropic scintillations are not still attenuated, and they are presented with practically the full weight. This range is the worst for chromatic correlation. In the range of rather skew occultations  $45 \leq \alpha < 85\text{--}88^\circ$ , the situation with the correlation of the scintillation components is analogous to that considered above, but the isotropic component is already significantly attenuated due to the frequency selection with averaging of signals in a sample and the suppression by filters. The anisotropic scintillations are considerably "riddled" of the isotropic ones, and the correlation is quite significant even with the fivefold increased weight of the isotropic component (curve 2). Note that for such skew occultations the weight of isotropic scintillations can be further suppressed by the additional time averaging

of the signals, because the anisotropic (correlated) component is shifted into the low-frequency region. The range of the angles here is wide enough, and such measurements seem to be most promising in the problems of global monitoring. In the range  $\alpha > 85\text{--}88^\circ$ , the correlation decreases (because it is low for anisotropic scintillations as well), and this range of angles is of no interest for the problem under consideration.

Note that in the range  $30 \leq \alpha < 85^\circ$  the correlation (and coherence) for the height of 30 km (curve 1) is much higher than for 40 km (curve 3). This is connected not only with the different weight ratio between the anisotropic and isotropic components of inhomogeneities at these heights, but also, to the greater extent, with the effect of filters, whose role increases fast with the decreasing height.

Consider now the problem of investigating into the parameters of anisotropic and isotropic scintillations with the following retrieval of the statistical characteristics of inhomogeneities. For this problem, the skew (including vertical) occultations  $\alpha > 45\text{--}60^\circ$  are most promising as well. This is connected with the fact that for close-to-vertical occultations the scintillations of both types superimpose and mask each other (curve 1 in Fig. 4a). When using skew occultations, the frequency selection allows analyzing the characteristics of anisotropic and isotropic scintillations separately. For anisotropic scintillations, the additional advantage is the fact that at a slant scanning of atmosphere, filters suppress the amplitude of isotropic scintillations in the whole frequency region, decreasing the contribution of isotropic scintillations in the frequency range, in which anisotropic scintillations are mostly concentrated. The degree of suppression of isotropic scintillations can be taken into account using the known characteristics of the effective filters and the regular profile of the refractive index. Finally, the effectively horizontal occultations allow estimating the anisotropy coefficient for anisotropic inhomogeneities.

## Conclusions

In this paper, we have analyzed the model coherence spectra and the correlation functions of chromatic stellar scintillations upon synchronous transmission through the Earth's atmosphere at separated wavelengths. In our calculations, we used the model 3D spectrum of relative fluctuations of the refractive index, developed based on the observations of stellar scintillations from the Mir station. The model 3D spectrum includes two components: one describing the properties of anisotropic, relatively large-scale inhomogeneities and another describing isotropic inhomogeneities. The anisotropic component of the spectrum of inhomogeneities is based on the model of saturated internal waves, and the isotropic component is described by the model of Kolmogorov turbulence. The calculations were performed in the approximations of the equivalent phase screen and weak scintillations. For low-orbit space vehicles (Mir station, ENVISAT/GOMOS, UVISI), the

approximation of weak scintillations is true for the ray perigee height of 30 km and higher.

The effect of the measurement conditions (observation geometry, wavelength separation, effective filters, sampling frequency of signals) on the spectra of chromatic scintillations has been analyzed. It has been shown that the coherence spectra allow refining the ranges of the angles of effectively vertical and effectively horizontal occultations. To study the structure of atmospheric inhomogeneities, of greatest interest are skew occultations, which provide for the frequency selection of anisotropic and isotropic scintillations, thus allowing their separate analysis. For anisotropic inhomogeneities, the coherence spectra and autospectra obtained at the effectively horizontal observations can be used to estimate the anisotropy coefficient  $\eta$ , the structure characteristic  $C_W$ , and the characteristic inner scale  $l_W$ . However, in the tangential occultation, the horizontal cross section is realized only in a small range of heights near the point of minimum  $h_{\min}$ . The effectively vertical occultations allow, in every observation session, the retrieval of the vertical profiles of the inner and outer scales, as well as the structure characteristic (the last is possible with some additional information about the anisotropy coefficient<sup>11</sup>), but carry no information about the anisotropy coefficient. For isotropic inhomogeneities, autospectra of scintillations permit retrieving the vertical profiles of the structure characteristic  $C_W$  and the inner scale  $l_K$  (if  $l_K \geq \rho_F$ ). Thus, the combination of the autospectra and coherence spectra for different atmospheric cross sections provides for estimation of all basic parameters entering into the model 3D spectrum of inhomogeneities (1)–(3).

The highest correlation of chromatic scintillations can be obtained for purely vertical and close-to-vertical occultations, for which the condition of effective verticality is fulfilled for both anisotropic and isotropic inhomogeneities. However, this range of angles is very small (only few degrees for the perigee height ranging from 30 to 40 km). Therefore, for mass observations, of greatest interest are skew occultations with  $45 \leq \alpha < 85\text{--}88^\circ$ , for which the anisotropic scintillations are still highly correlated, and the contribution of isotropic (uncorrelated) scintillations is significantly suppressed by the frequency selection and filters. The weight of isotropic scintillations can be additionally suppressed by the following time averaging of signals. The use of the information about the properties of correlation between scintillations at different wavelengths allows the errors associated with the scintillation noise to be reduced when retrieving the content of the atmospheric constituents in the satellite spectrometric method of star transmittance. From the time shift corresponding to the maximum of the mutual correlation function, it is possible to determine the dispersion shift of rays in the atmosphere and to retrieve the regular vertical profile of the refractive index (and, consequently, density and temperature), using the Abel inversion.

The synchronous sensing of the atmosphere at two wavelengths significantly extends the capabilities

of the satellite stellar scintillation method for investigation of parameters of the small-scale structure of density inhomogeneities. The analysis of spectra and correlation functions of chromatic scintillations permits developing an optimal strategy of satellite experiments for monitoring of the statistical structure of inhomogeneities and the content of atmospheric constituents.

### Acknowledgments

The author is grateful to A.S. Gurvich for useful criticism and discussions.

This work was supported, in part, by the Russian Foundation for Basic Research (project No. 03–05–64366) and CNRS (project No. 16340).

### References

1. G.M. Grechko, A.S. Gurvich, V. Kan, S.A. Savchenko, and A.I. Pakhomov, *Atmos. Oceanic Opt.* **14**, No. 12, 1026–1037 (2001).
2. G.M. Grechko, A.S. Gurvich, V. Kan, A.I. Pakhomov, Ya.P. Podvyaznyi, and S.A. Savchenko, *Dokl. Ros. Akad. Nauk* **357**, No. 5, 683–686 (1997).
3. A.S. Gurvich, *Dokl. Ros. Akad. Nauk* **385**, No. 2, 242–246 (2002).
4. A.S. Gurvich, V. Kan, S.A. Savchenko, A.I. Pakhomov, P.A. Borovikhin, O.N. Volkov, A.Yu. Kaleri, S.V. Avdeev, V.G. Korzun, G.I. Padalka, and Ya.P. Podvyaznyi, *Izv. Ros. Akad. Nauk, Fiz. Atmos. Okeana* **37**, No. 4, 469–501 (2001).
5. A.S. Gurvich and V. Kan, *Izv. Ros. Akad. Nauk, Fiz. Atmos. Okeana* **39**, No. 3, 335–358 (2003).
6. J.F. Carbary, E.H. Darlington, T.J. Harris, P.J. McEvadady, M.J. Mayr, K. Peacock, and C.I. Meng, *Appl. Opt.* **33**, No. 9, 4201–4213 (1994).
7. "The European Space Agency's GOMOS, MIPAS and SCIAMACHY Calibration and Verification Teams. ENVISAT taking up duty of atmospheric composition sounding," *SPARC Newsletter: Stratospheric Processes and Their Role in Climate*, No. 19, 5–10 (2002).
8. F. Dalaudier, V. Kan, and A.S. Gurvich, *Appl. Opt.* **40**, No. 6, 866–889 (2001).
9. V.A. Polyakov, Yu.M. Timofeev, A.S. Gurvich, V.V. Vorob'ev, V. Kan, and J.-H. Yee, *Izv. Ros. Akad. Nauk, Fiz. Atmos. Okeana* **37**, No. 1, 56–66 (2001).
10. V.A. Polyakov, V.V. Vorob'ev, and V. Kan, *Izv. Ros. Akad. Nauk, Fiz. Atmos. Okeana* **38**, No. 2, 175–181 (2002).
11. A.S. Gurvich and V.L. Brekhovskikh, *Waves in Random Media* **11**, No. 3, 163–181 (2001).
12. *Geophysics Handbook* (Nauka, Moscow, 1965), 572 pp.
13. A.S. Gurvich, *Izv. Vyssh. Uchebn. Zaved., Radiofiz.* **27**, No. 8, 951–959 (1984).
14. V.I. Tatarskii, *Wave Propagation in a Turbulent Medium* (Mc Graw-Hill, New York, 1961).
15. A.S. Gurvich and I.P. Chunchuzov, *J. Geophys. Res.* (in print).
16. A.A. Volkov, G.M. Grechko, A.S. Gurvich, V. Kan, and S.A. Savchenko, *Atm. Opt.* **3**, No. 8, 806–811 (1990).
17. G.M. Grechko, A.S. Gurvich, V. Kan, S.V. Kireev, and S.A. Savchenko, *Adv. Space Res.* **12**, No. 10, 169–175 (1992).
18. J.S. Bendat and A.G. Piersol, *Random Data Analysis and Measurement Procedures* (Wiley, New York, 1971).
19. S.M. Rytov, Yu.A. Kravtsov, and V.I. Tatarskii, *Introduction to Statistical Radiophysics. Part 2. Random Fields* (Nauka, Moscow, 1978), 464 pp.